Line of Sight Stabilization of a Gimbaled Mechanism Under Passive Base Isolation

Kutlu Demir KANDEMİR and Dr.Yiğit YAZICIOĞLU** and Dr. Alper AKMEŞE****

*TÜBİTAK-SAGE

kutlu.kandemir@sage.tubitak.gov.tr

**Middle East Technical University

yigit@metu.edu.tr

***TÜBİTAK-SAGE

alper.akmese@sage.tubitak.gov.tr

Abstract

Line of Sight (LOS) stabilization is an important concept for aerospace applications utilizing gimbaled imaging systems. A widely used method for protecting the LOS stabilization system from the disturbing effects of the base vibrations is to mount it on passive vibration isolators. However, these isolators may interact with gimbal controller and drastically limit the stabilization performance. This work deals with LOS stabilization problem in aerospace structures by focusing on the parameters of controller and vibration isolation system. The problem is investigated on an experimental setup for a specific case. Several performance tests are applied on the setup and results are used to generate design constraints.

1. Introduction

1.1 Gimbal mechanism

The gimbal mechanism is mainly used to adjust the angular orientation of an object with respect to another body or inertial space. This object could be an antenna, an inertial stabilization platform (ISP) or an imaging system. So, the gimbal mechanism has a wide area of use in aviation, military, telecommunication and imaging applications [1].

Gimbaled systems are composed of rotary joints; therefore the parameters to be sensed are generally angular position and its time derivative with respect to inertial frame. In gimbaled stabilization systems, commonly used position sensors are potentiometer, encoder and resolver [2]. When properly aligned, gyroscopes can be utilized as angular rate sensors for gimbal mechanisms [3]. A gyroscope generates an output which is proportional to the instantaneous angular speed of its measurement axis with respect to the Earth.

Considering the actuation mechanism, a gimbal can be actuated via direct drive, gear-driven, or mechanism driven methods. Where, modern, commercially available gimbals almost always use direct-drive or gear-driven servo motors to actuate the joints. Due to the physical limitations of the cables, many of these mechanisms are constrained to a reduced operational region. While more sophisticated models use a slip ring to allow continuous rotation about an axis [4].

1.2 Line of Sight Stabilization

Line of Sight (LOS), being the most important parameter of pointing and tracking systems, is defined as an imaginary line along which an observer perceives. Depending on the type of application, The LOS can be the aim point of a beam or weapon, the center of the field of view (FOV) of an airborne camera, or the direction a sensor is pointed [1]. Accordingly, LOS stabilization can be expressed as the act of keeping this imaginary line at a desired orientation under the effect of external disturbances such as joint frictions or base structure vibrations etc. Thus, LOS stabilization is a question of attenuating disturbances [3] [5].
Since the LOS stabilization is related to adjusting angular orientation of a system, gimbal is the best and most widely used mechanism for this purpose.

LOS stabilization systems are classified into two groups according to how the angular rate of the gimbal axis is calculated. If the stabilization task is achieved by using the angular rates taken from the gimbal base, such systems are called strap down stabilized or pseudo referenced stabilization systems. This topology requires estimation of gimbal axis rates based on the measurement taken from the base platform. On the other hand, placing the rate sensor on the gimbal axis yields the LOS rates directly. This method is called as true referenced pointing [6] [7]. Figure 1 illustrates a true referenced gimbaled LOS stabilization system.

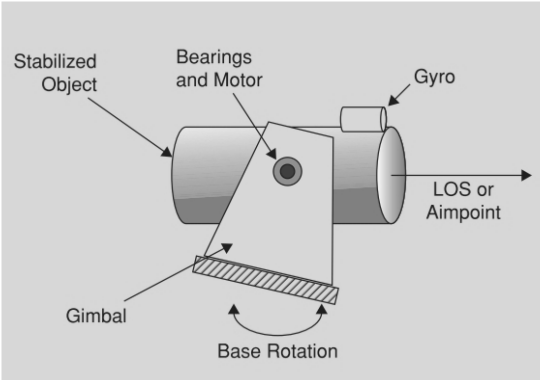

Figure 1 - Gimbaled LOS stabilization system [1].

The definition of LOS stabilization brings in two different tasks to be achieved together in terms of controls, which are tracking and stabilization. Tracking can be expressed as the act of bringing the LOS to the desired angle. Since it is an orientation problem, main control variable is the angular position of the gimbal axis. Tracking is achieved by observing angular position and generating proper torque commands. The second control task, namely stabilization, is defined as keeping the LOS at desired orientation under the effect of base motion and/or other disturbances like jitter, alternatively keeping the rate of pointing error at zero. Therefore, it is achieved by observing angular velocity with respect to inertial reference frame and actuating the gimbal accordingly.

Most LOS stabilization controllers use an inner stabilization loop inside an outer tracking loop. The inner stabilization loop compensates for disturbances and minimizes unnecessary motion of the payload. Meanwhile, the outer tracking loop ensures that LOS points the desired orientation [8].

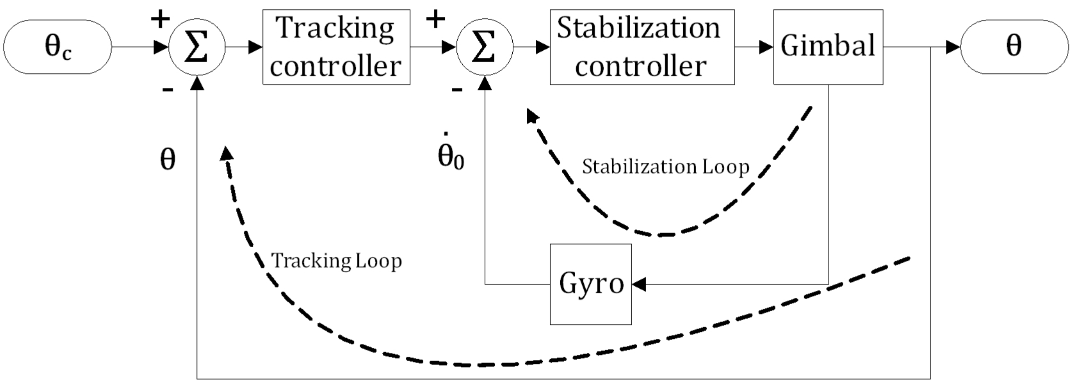

Figure 2 - Typical LOS stabilization controller topology.

Those feedback loops work on different reference frames. In other words, the stabilization loop measures the angular velocity of the gimbal with respect to inertial frame (denoted with θ_o in Figure 2), whereas the tracking loop measures the angular position with respect to the gimbal base. Yet both loops share the only control variable, motor torque command. Although being distinct control tasks, tracking and stabilization has to be combined in a suitable way. Inevitably, a compromise must be accomplished between stabilization and tracking in the control design stage. Stabilization loop has to be fast enough to attenuate disturbances and also has to be responsive to the tracking commands coming from the outer loop. Consequently it has a greater bandwidth compared to tracking loop.

1.3 Passive Vibration Isolation

The aim of vibration isolation is to protect a system from self induced or external dynamic forces. Due to its simplicity and low cost, passive isolators are usually preferred. These components act as a low pass filter by damping out the high frequency vibration of the base structure and transmitting only low frequency motions.
Vibration isolation systems have to comply with contradictory requirements such as stiffness reduction for better isolation and stiffness increase for better performance [9]. This is valid for any dynamical system which utilizes isolators to be protected from external or self excited vibrations. For instance, the isolated object can be the inertial measurement unit of an airplane, or a CNC grinding tool.

Vibration isolation is a requirement for LOS stabilization systems including vibration sensitive components. It is realized by mounting several isolators to suitable places between the gimbal frame and base. Therefore the locations and type of these isolators have great impact on stabilization performance.

1.4 Problem definition

Consider a single axis gimbaled LOS stabilization mechanism whose base is mounted to the ground with passive vibration isolators. If the control effort applied to point the payload of the gimbal excites the flexible modes of the base isolation, it can destabilize the system or cause enough ringing to prevent meeting pointing stability requirements [10]. This is known as control structure interaction (CSI) problem.

In literature, there exist various methods to deal with this problem. For instance, CSI can be formulated as a robust performance problem, modeling structural interactions as uncertainties in the feedback loop and updating the controller [11]. In addition, using notch filters in the feedback loop is another method of dealing with CSI. However it brings a phase lag and limits the bandwidth of the system to one-third of the structural natural frequencies [1]. It is also seen that when structural resonances within the system bandwidth are inevitable, they can be expressed in the form of a mass-spring-damper and included in the mathematical model of the gimbal [12].

The proposed solutions bring an extra workload to the control designer, by limiting the system performance and/or requiring complex mathematical modeling. Also it has to be noted that they are case specific. The control system might not be able to tolerate the additional phase lag or gain, which is caused by the elements brought into the loop. It might be the case that, even if there is a structural mode within the controller bandwidth, actuation forces can be too small and do not cause a significant interaction. Therefore, it is beneficial to verify the existence of CSI with experimental methods, before trying to solve it.

This work focuses on the interaction between a LOS stabilization system and its base isolation with experimental methods. A test setup, which allows changing base isolation parameters and stabilization controller bandwidth, is designed. Stabilization performance is observed by exposing that setup to several different vibratory conditions. The relation between controller bandwidth and base isolation and their effect on stabilization performance is sought.

2. Theory and Formulation

The starting point is to obtain kinematic expressions for the gimbal and base isolation. There are some basic assumptions that should be clarified before;

First of all, the gimbal is assumed to be axisymmetric and balanced along its rotation axis. Besides, the joint properties are assumed to be linear and time invariant. They will be modeled with simple inertia, rotary spring and rotary viscous damper. Any nonlinear behavior like hysteretic damping or coulomb friction is omitted [13], [14].

Kinematically, the experimental setup is a serial manipulator which includes three links and two revolute joints. A schematic illustration of the links and joints are given in Figure 3.

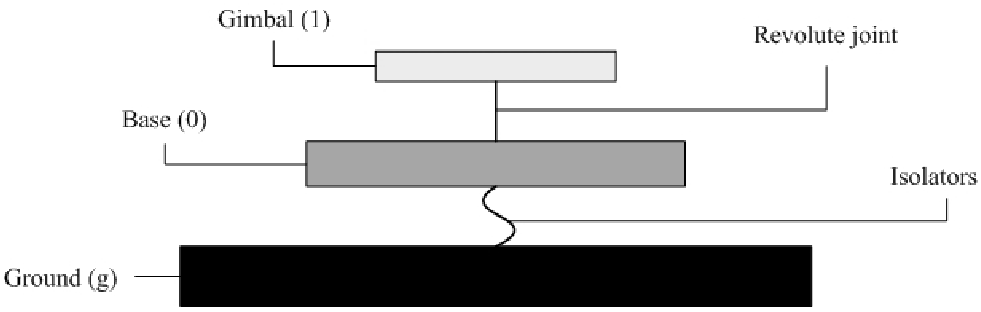

Figure 3 – Schematic expression of the links and joints.

Equation of motion for the base plate and gimbal axis are given as follows:

$$(J_0 + J_1)\ddot{\phi} + c_{t0}\dot{\phi} + k_{t0}\,\phi = -T_\theta \tag{1}$$

$$J_1\ddot{\theta} + c_{t1}\dot{\theta} + k_{t1}\theta = T_\theta \tag{2}$$

Where:

J_0 : inertia of the base plate

J_1 : inertia of the gimbal axis

c_{t0} : equivalent rotary viscous damping of the isolators

k_{t0} : equivalent rotary stiffness of the isolators

ϕ : base plate rotation angle

c_{t1} : equivalent rotary viscous damping of the revolute joint

k_{t1} : equivalent rotary stiffness of the revolute joint

θ : gimbal rotation angle

T_ϕ : gimbal motor torque

Note that the input torque is exerted by gimbal motor and has the same magnitude and opposite direction in equations 1 and 2.

Another behavior which has to be formulated is the adjustable isolation natural frequency. It is realized by changing the position of four elastomeric isolators. Consequently, relation between isolator locations and isolation natural frequency has to be determined. The axis of rotation for the first rotary mode of the isolated system should be parallel to the gimbal axis and should be adjustable such that, it can be set to desired values.

Rivin presents a 2-D model of a bar which is connected to base through two parallel linear springs. The bar rotates along y direction with an angle of θ. For small rotations, the equivalent angular stiffness is expressed as follows [9]:

$$\frac{M}{\theta} = Kt_{eq} = (k_1\ a_1{}^2 + k_2\ a_2{}^2) \tag{3}$$

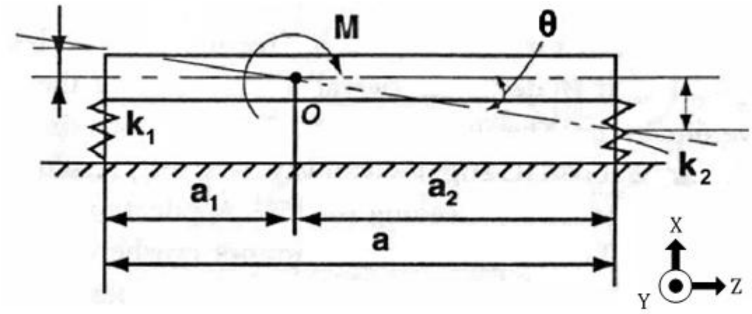

Figure 4 - Equivalent angular stiffness of a bar mounted with linear springs [9].

If the spring constants are equal and moment is applied at the middle of the plate then the expression reduces to:

$$Kt_{eq} = \frac{k\,a^2}{2} \qquad 4$$

From which, the rotary natural frequency of the bar can be obtained simply as follows

$$\omega_{n\,\theta} = \sqrt{\frac{Kt_{eq}}{I_y}} = \sqrt{\frac{k}{2\,I_y}}\,a \qquad 5$$

Where:

I_y : inertia of the bar about y axis

Kt_{eq} : equivalent angular stiffness

a : distance between isolators

k : isolator stiffness

$\omega_{n\,\theta}$: angular natural frequency about y axis

Equation 5 explains that, rotary natural frequency of the bar is directly proportional to the distance between isolators.

This approach can be extended to a planar vibration isolation system where a rectangular plate is connected to ground with four isolators. In order to avoid interactions between different structural modes, the first controlled rotary mode should be separated and shifted to lower frequencies from the rest. This can be obtained by adjusting the isolator stiffness and the perpendicular distance between them. Figure 5 illustrates an isolator configuration which successfully decreases the angular natural frequency along Y direction.

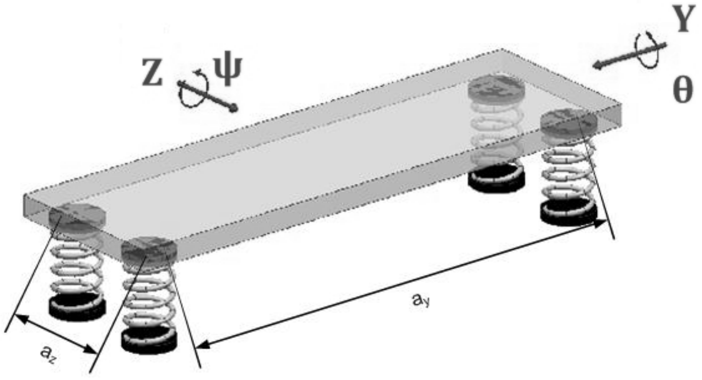

Figure 5 - Planar vibration isolation

The last design detail to be explained is controller. It is aimed to obtain a set of LOS stabilization controllers having different bandwidths. In control theory, bandwidth of a closed loop control system is defined as; the frequency range, in which the ratio of input and output is between ±3 dB and phase difference is less than 90°.

Any LOS stabilization controller that meets the above definition is regarded as successful. Therefore, the aim in controller design is not to obtain the best response, but to reach a sufficient stabilization bandwidth. This moderate requirement somewhat simplifies the controller topology. Consequently, a two-loop cascaded controller which includes an inner stabilization loop and an outer tracking loop is selected (see Figure 2). It is decided to use a PI controller for the tracking loop, and PID with approximate derivative for the stabilization loop.

3. Experimental Setup

Previous section presented design guidelines for the experimental setup. Equation of motion is obtained in symbolic form and several structural design limitations are set. In addition, gimbal controller topology is determined. This part is devoted to realization and verification of the experimental setup based on those guidelines.

3.1 Sensors and actuators

Gimbal's angle with respect to the base is indicated by a brushless type resolver having a resolution of 60 arc-second. Absolute angular velocity of the gimbal is measured by a MEMS gyro that has 110 Hz bandwidth and ±200°/sec range.

Third and the last sensing task is measuring the angular position of gimbal base plate with respect to ground. The joint between these two links is composed of elastomeric vibration isolators, which primarily allow for rotation, but also let a small amount of translation. Therefore, conventional angular position sensors are not suitable. In order to filter out the effect of linear displacement, two equally spaced laser distance sensors working at 1 kHz, each looking downwards, are placed at both sides of the base plate. This configuration enables measurement of the base plate rotation by filtering out the effects of translational movements and provides a resolution of 0.002 degrees. Distance readings are converted to angle data by using equation 6. This measurement concept is illustrated in Figure 6.

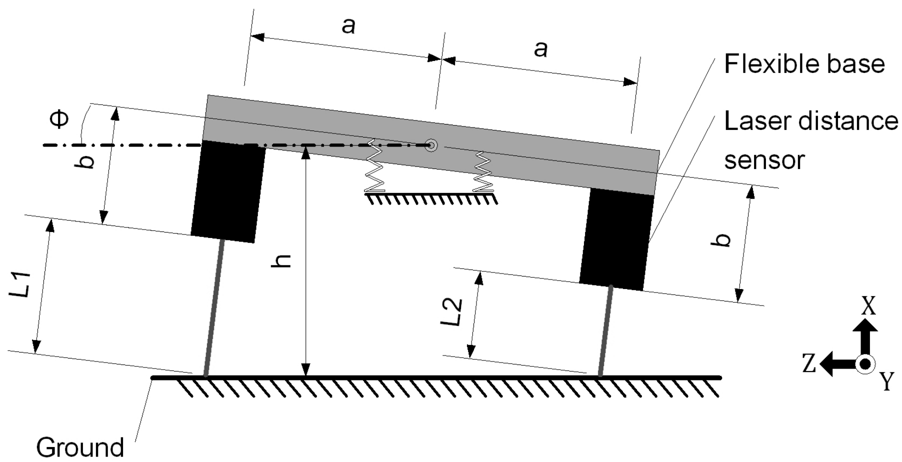

Figure 6 - Laser distance sensors at tilted condition

$$\Phi = \mathrm{ATAN2}\left((L1 - L2), (2a)\right) \tag{6}$$

L1 and L2 designate distance measurements.

The only actuator is a single frameless brushless DC motor which is placed at the end of the gimbal. It has a maximum torque of 0.141 Nm and driven by a PWM servo amplifier having 33 kHz switching frequency.

Commutation is provided by the internal Hall Effect sensor.

3.2 Structural design

Main aim in structural design is to obtain an adjustable rotational mode for the base isolation. In section 2, it is expressed that, this can be achieved by adjusting the lateral distance between isolators. Hence, the setup is designed such that the isolators are connected to movable brackets, whose perpendicular distance can be set to different values. Figure 7 is taken from a computer aided modeling program and illustrates this concept. The brackets can be mounted to different set of holes, resulting in an adjustable angular natural frequency.

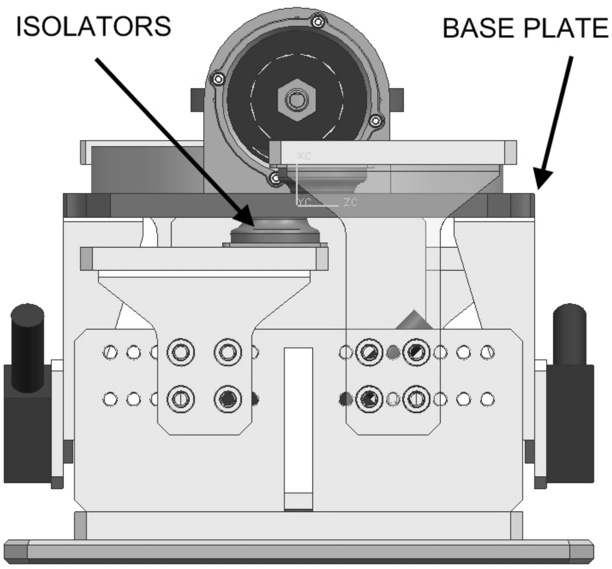

Figure 7 - Side view of the setup

Three different isolator configurations are selected to be used in the performance tests. For each, attainable natural frequencies are calculated by equation 5. Besides a random vibration test is conducted for verification. Results are tabulated as follows:

Table 1 - Attainable base isolation natural frequencies

	Theoretical Calculation	Random Vibration Test
Configuration 1	7 Hz	17.5 Hz
Configuration 2	14 Hz	30 Hz
Configuration 3	21 Hz	42.5 Hz

The significant difference between theoretical calculation and test results can be explained by the neglected nonlinearities of the isolators. Besides, equation 5 neglects lateral and angular stiffness constants of the isolators. However, in reality they have a significant effect on the dynamic behavior of the overall system.

3.3 Controller design

First step of controller design is determining the plant parameters. Using MATLAB System Identification Toolbox™, equation 1 is expressed in state space form. Inertia, damping and stiffness are defined as estimation parameters. A random torque is applied to the gimbal and corresponding input and outputs are fed to the readily available parameter estimation function in System Identification Toolbox™. Results are given in Table 2.

Table 2 - Parameter estimation results

	Value	Unit
J_1	1,59 x 10^{-4}	kg-m^2
c_{t1}	0.0021	N m/rad-s
k_{t1}	0.0157	N m/rad

According to the design guidelines, stabilization controller bandwidth is another parameter that has to be varied in performance tests. For this purpose, three different stabilization controllers are designed. Their bandwidths are selected to be 15, 30 and 45 Hz respectively. Note that these values are almost equal to the attained structural natural frequencies. The tracking controller bandwidth is set to 5 Hz.

In section 2, the tracking and stabilization controllers are selected to be of PI and PID type respectively. They are expressed in Laplace domain as follows:

$$G_{CS}(s) = K_p + \frac{K_i}{s} + \frac{K_d\, s}{\frac{1}{n}s + 1} \quad (7)$$

$$G_{CT}(s) = K_p + \frac{K_i}{s} \quad (8)$$

Controller parameters are tuned for the desired closed loop bandwidths. Results are given in Table 3 and 4 respectively

Table 3 - Stabilization controllers

	Controller 1 (15 Hz BW)	Controller 2 (30 Hz BW)	Controller 3 (45 Hz BW)
K_i	0.170	0.949	3.442
K_p	0.217	0.376	0.522
K_d	-1.3 x 10^{-3}	3.52 x 10^{-4}	1.98 x 10^{-3}
n	80.004	1538	32228

Table 4 - Tracking controller

	Controller 1 (5 Hz BW)
K_i	132.954
K_p	26.816

Controllers are realized by XPC Target™ module of SIMULINK®. XPC Target™ is a dedicated computer utilizing proper interface boards which are connected to the sensors and actuators of the experimental setup. It is used for the hardware-in-the-loop (HWIL) simulation of the designed controller. Schematic drawing of the control system is shown in Figure 8.

The controller is designed in the host computer by MATLAB®, and then it is embedded in a control interface in SIMULINK®, and finally loaded to XPC Target™ through TCP/IP connection. Start/stop commands and reference inputs are given through the control interface in the host computer, while the controller is simulated in real time by the target computer.

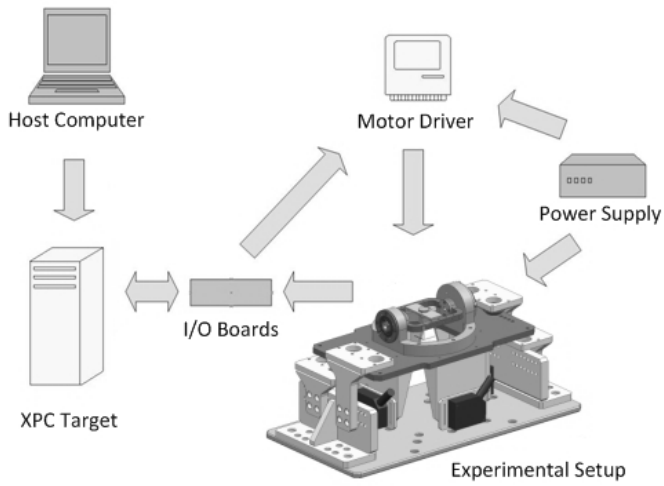

Figure 8 - Control system schematic

4. Tests and Results

The test will be applied with three controllers and three base isolation natural frequencies. Therefore totally nine different configurations exist. Resultant configuration matrix is presented in Table 5. Under a 2 g-rms random base vibration, a constant angle command is applied to the controller.

The primary measure for the tests is stabilization performance, which can be defined as the range of LOS error with respect to the inertial frame, during a specified time interval. In digital imaging systems, this duration corresponds to exposure time. Image quality of a stabilized camera is inversely proportional to the LOS error within exposure time.

Table 5 - Test matrix

Isolator configuration	Controller 1 (15 Hz BW)	Controller 2 (30 Hz BW)	Controller 3 (45 Hz BW)
Config 1 (17.5 Hz)	Test 1	Test 4	Test 7
Config 2 (28 Hz)	Test 2	Test 5	Test 8
Config 3 (42.5 Hz)	Test 3	Test 6	Test 9

The experimental setup enables two ways to find LOS error. First, it can be calculated by adding up the position data measured by the resolver and laser distance sensors; second, it can be evaluated by integrating the gyroscope output. Since the gyroscope has a higher bandwidth compared to the resolver, latter method is preferred.

An exposure time of 10 milliseconds is selected. Limits of the LOS error are calculated for each 10 millisecond interval that can be taken out from the data. Root-mean-square (rms) of this data will indicate the stabilization performance. Note that smaller the rms LOS error, better the stabilization performance is.

Results are presented in a 3-D bar chart in Figure 9. The bottom axes represent the isolator configuration and closed loop bandwidth of stabilization loop and the vertical axis represents the rms LOS error for the corresponding test.

First implication of Figure 9 is that, the primary factor in stabilization performance is the stabilization controller bandwidth. Regardless of the base isolation natural frequency, an increase in stabilization controller bandwidth decreases the LOS error.

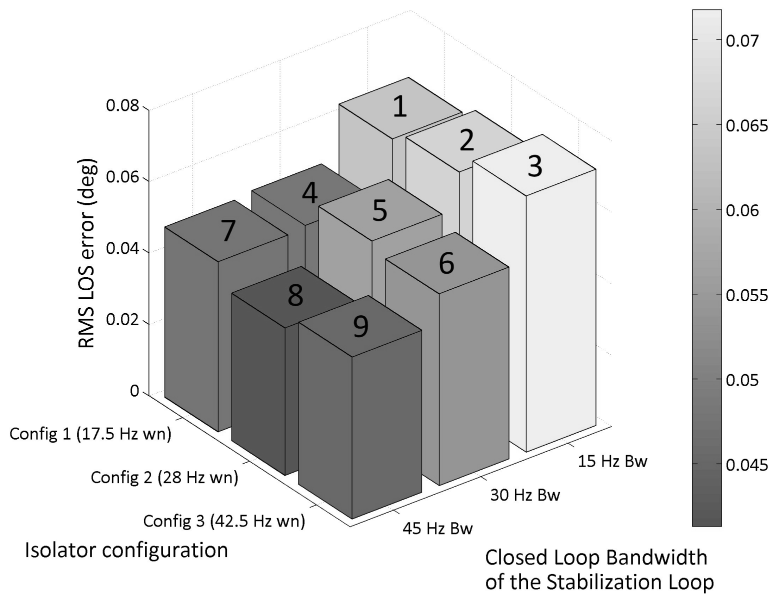

Figure 9 - Test results

Focusing on the bottom and top values, it can be seen that Test 3 yields the worst and Test 8 yields the best performance. Comparing the relative locations of controller bandwidth and isolation natural frequency for these two tests, it can be seen that, as stabilization controller bandwidth falls below of the isolation natural frequency, stabilization performance gets worse. Therefore it can be concluded that, for this configuration, keeping the bandwidth larger than structural natural frequency yields a better stabilization performance.

The results are interesting in terms of showing no evidence of an apparent interaction between controller and structure. Although Tests 1, 5 and 9 are prone to CSI by having nearly equal controller bandwidths and natural frequencies, they do not show significant performance degradation compared to the others. In fact, Test 1 has the best performance among the cases with 15 Hz controller bandwidth.

Yet, it is beneficial to note that, sampling of the tests remains too coarse to be conclusive for CSI analysis. Using a finer mesh for controller bandwidth and structural natural frequency would give a better idea on this subject.

5 Conclusion

This was an interdisciplinary work on stabilization systems, starting from the kinematic analysis, structural design and going up to controller design and performance verification. The problem definition necessitates construction of an experimental setup on which controller structure interaction parameters are studied.

For the given set of isolators and gimbal, it is concluded that;
When base isolation natural frequency is pushed down to comparable frequencies with stabilization controller bandwidth, the relative position of these two parameters does affect the stabilization performance. Placing the structural natural frequency below the closed loop stabilization controller bandwidth, yields better stabilization performance.

Another important outcome of this work is the experimental setup itself, which is built for this analysis. In future, it is possible to conduct controller structure interaction analyses, with different isolator and gimbal configurations.

Lastly, as a future work, attaching a camera inside the gimbal and using its image quality as the performance measure would be a more realistic stabilization analysis.

References

[1] Hilkert, J. M. (2008). Inertially Stabilized Platform Technology. IEEE Control Systems Magazine, (February), (pp.26-46).

[2] Nalbantoglu, V., & Seymen, B. (2008). Gyro-Bias Estimation Filter Design for the Stabilization Accuracy Enhancement of Two Axes Gimbaled Sighting Systems. 17th World Congress; The International Federation of Automatic Control, (pp. 5011-5017).

[3] Yoon, S., & Lundberg, J. (2001). Equations of motion for a two-axes gimbal system. IEEE Transactions on Aerospace and Electronic Systems, 37(3), 1083–1091. Retrieved from http://ieeexplore.ieee.org/xpls/abs_all.jsp?arnumber=953259.

[4] Osborne, J., Hicks, G., & Fuentes, R. (2008). Global analysis of the double-gimbal mechanism. IEEE Control Systems Magazine, 28(4), (pp.44–64).

[5] Wongkamchang, P., & Sangveraphunsiri, V. (2008). Control of Inertial Stabilization Systems Using Robust Inverse Dynamics. Thammasat International Journal of Science and Technology, 13(2), 20-32.

[6] Becker, G., Cubalchini, R., Tham, Q., & Anagnost, J. (1999). Generation of structural design constraints for spaceborne precision pointing systems. In Control Applications, 1999. Proceedings of the 1999 IEEE International Conference on (Vol. 1, pp. 69-74).

[7] Rudin, R. (1993). Strapdown stabilization for imaging seekers. Second Annual AIAA SDIO Interceptor Technology Conference.

[8] Masten, M. (2008). Inertially stabilized platforms for optical imaging systems. IEEE Control Systems Magazine, 28(1), (pp. 47-64).

[9] Rivin, E. I. (2003). Passive Vibration Isolation. New York.

[10] Spanos, J. (1989). Control-structure interaction in precision pointing servo loops. Journal of Guidance, Control, and Dynamics, 12(2), (pp.256–263).

[11] Balas, G. J., & Young, P. M. (1995). Control Design for Variations in Structural Natural Frequencies, Journal of Guidance, Control and Dynamics, 18(2), 325-332

[12] Profeta, J., Vogt, W., & Mickle, M. (1990). Torque disturbance rejection in high accuracy tracking systems. IEEE Transactions on Aerospace and Electronic Systems, 26(2), (pp.232-287).

[13] Waldmann, J. (2002). Line-of-Sight Rate Estimation and Linearizing Control of an Imaging Seeker in a Tactical Missile Guided by Proportional Navigation. IEEE Transactions on Control Systems Technology, 10(4), 556-567.

[14] Lee, T. H., Koh, E. K., & Loh, M. K. (1996). Stable adaptive Control of multivariable servomechanisms, with application to a passive Line-Of-Sight stabilization system. IEEE Transactions on Industrial Electronics, 43(1), (pp.98-105).